Bubble size measurement in flotation column – numerical or imaging method

Z. JAVOR AND L.O. FILIPPOV*
Université de Lorraine, GeoRessources, CNRS, UMR 7359, 2 rue du Doyen Marcel Roubault, TSA 70605 France
Corresponding author: lev.filippov@univ-lorraine.fr

Abstract

Easy bubble size regulation defines an efficient control of flotation column and renders it as economic processing way to recover the fine mineral particles. Strong interaction occurs between superficial gas (J_g) and feed velocities (J_l) for bubble size. The optimum operating conditions must accordingly be maintained to prevent the bubble coalescence leading to average bubble size increase or carryover of small bubbles into the tailings. This paper discusses the interaction between the parameters employed to characterize the dispersion of the sparged air. The differences of the two majors bubble size analysing techniques (bubble viewer and drift flux model) are also investigated. Four different approaches using the drift flux analysis are compared with experimental data collected from a 5,5 m height pilot flotation column. The changes of bubble size as a function of column height in frother and salt solution are also reported. The advantages of the numerical method are highlighted.

INTRODUCTION

Bubble column reactor is a multiphase contactor where gas comes into contact with liquid or liquid-solid (slurry) system, which is widely used in chemical (e.g. oxidation, polymerization, chlorination etc.), petrochemical, biochemical (e.g. wastewater treatment, fermentation), and mineral processing (Kantarci et al., 2005; Shah et al., 1982). The main advantages of these rectors are the low operation and maintenance costs, the compact design, the easy operation, the adjustable residence time and the high heat and mass transfer rate (Shah et al., 1982).

Bubble column reactor has been successfully used in mineral processing industry since the early 80's, particularly in the cleaning phase of flotation circuit. Bubble column reactor used in the flotation process is most commonly called flotation column. Compared to the mechanical flotation cells the flotation columns are more effective with fine particles, has lower capital and operation cost due to lack of moving parts, has less floor space demand, and it is easier to control automatically. It is extensively used for final cleaning in copper and zinc sulphide flotation, in molybdenite cleaning, phosphate flotation and iron ore flotation (Dobby, 2002).

During the flotation process the interacting phases are the continuous liquid phase and the dispersed gas and solid phase. The liquid phase or medium is responsible for carrying the solid particles and also for providing a suitable chemical environment for the successful process. The solid phase is the one to be separated and removed from the liquid phase while the actual separation process is fulfilled by the gas phase (bubbles). The air is sparged into the slurry at the bottom of the column and the buoyancy force makes the bubbles rise to the top of the cell while colliding with mineral

particles that can attach to the bubbles and rise to the surface creating a mineralised froth phase. The efficiency of the process is strongly determined by the size and the velocity of the rising bubbles:

- the smaller the bubble the bigger the active surface area where particle-bubble collision can take place
- the slower the bubble rise velocity the longer the bubble residence time resulting longer particle-bubble interaction time (higher grade and selectivity can be obtained).

The parameters determine bubble size and velocity can be categorized into five major groups: column design, operation parameters, gas-phase-, liquid-phase- and solid-phase property.

THE FIVE MAJOR PARAMETERS AFFECT COLUMN OPERATION

Design parameters

Flotation columns consist of two distinct zones Figure 1: the collection zone, and the forth zone. The collection zone is between the feed zone where the particles are suspended in the water and the sparger technology where the air bubbles are dispersed into the water. In this zone bubble – particle collision, particle attachment and detachment takes place leading to the formation of bubble-particle aggregates that will rise up above the feeding zone to the froth zone forming mineralized froth phase.

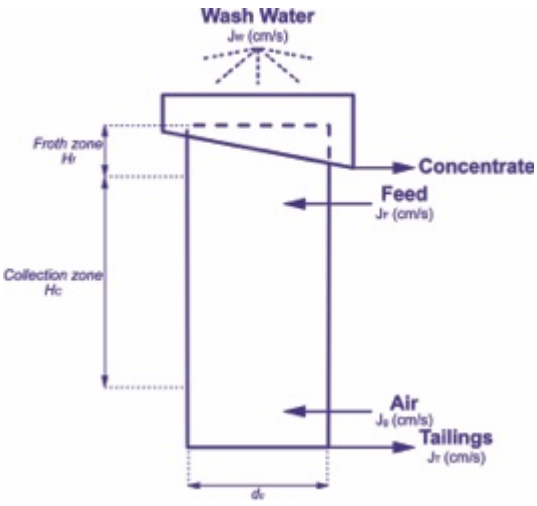


Figure 1. Schematic of flotation column [Based on (Dobby, 2002; Sastri, 1998)]

There are multiple sparger technologies used to disperse air into the column but they can be divided into two major groups: internal and external spargers. Industry prefers external sparger to internal one due to the cheaper and faster maintenance. Most widely employed industrial spargers are the Microcell™ (Metso), the CPT Slamjet® and the CPT CavTube™ (Eriez) (Wills and Finch, 2015). In Microcell™ (Metso) and CavTube™ (Eriez) the slurry that is extracted from the column is reintroduced via the sparger technology while air is mixed into the medium while the Slamjet® system forcing a high pressure air through a tube and jetting air into the slurry.

Industrial bubble columns usually operate with a length-to-diameter ratio (H:D). Typical height and diameter varies between 6 to 14 m and 0.5 to 5 m respectively (Finch and Dobby, 1990). Choosing the right length-to-diameter will have an effect on the gas-liquid surface area, axial dispersion

coefficient of gas and solid, bubble size, rising velocity and fluid dynamic (Pangarkar, 2015; Shah et al., 1982).

Operational parameters

This group collects all of the parameters that can be directly controlled or regulated during the measurement, e.g. volumetric gas flow rate (Q_g), volumetric liquid flow rate (Q_l), operational temperature and pressure, solid to liquid portion in slurry etc. The increase of Q_g will enhance the volume of dissolved air in the continues phase however its effect on the size distribution and rising velocity of the bubbles is strongly determined by the property of the liquid phase. Since most of the flotation column used in mineral processing is counter-current column the increase in Q_l will have a significant effect on the rising velocity of the bubbles. The operational pressure or the operation temperature can not be as easily regulated as Q_g or Q_l but both have a significant effect on bubble size and rising velocity so these parameters have to be considered during column operation. Both operational temperature and operational pressure tends to decrease bubble size as they increasing. The increase of operational temperature decreases liquid velocity leading to smaller bubble size while the increase of operational pressure increases the gas density leading to smaller bubble size (Schafer et al., 2002). The efficiency of froth flotation is strongly influenced by the solid concentration that usually varies between 25 to 40% (COCHILCO, 2009). Increasing the solid concentration reduces liquid viscosity leading to more frequent bubble coalescence and therefore to increased bubble size (Kara et al., 1982; Kato et al., 1972; Pino et al., 1992).

Gas phase property

Gas density (ρ_g) has a pronounced effect on bubble size and hence on bubble rising velocity (Schafer et al., 2002). The increasing gas density increases inertia forces in the bubbles leading to smaller stable bubble diameter.

Liquid phase property

There are three crucial properties affecting flotation performance: density, viscosity and water quality/impurity. The increase of liquid density or viscosity reduces the turbulence in the liquid phase leading to increased bubble size (Kantarci et al., 2005; Schafer et al., 2002). The complexity of the action of water quality on bubble properties cannot be explained in term of the usual viscosity, density or surface tension properties of the liquid (Pino et al., 1992). Certain impurities such as surface-active agent or dissolved electrolytes can diminish bubble size by preventing the coalescence between colliding bubbles. In case of surface-active agents (surfactant), the adsorbed molecules changes the boundary condition of air /liquid interface from slip condition to partial-slip or non-slip leading to slower drainage speed (Henry et al., 2007). The film thinning is conducted by such local hydrodynamic properties of the interface as surface elasticity and surface tension gradient. In case of dissolved electrolytes, the decrease of bubble coalescence frequency has been extensively studied but the phenomena responsible for the decrease is still not well understood. There are many different theories but none of them has the potential to fully explain the phenomena. The theories can be divided into three groups: colloidal force effects, ions specific effect on air/liquid interface properties and ion-pair effects. There are four colloidal forces associated with the bubble-bubble interactions the Van der Waals attraction force, the repulsive electrostatic double layer force (EDL), the attractive hydrophobic pressure and the repulsive hydration pressures. The attractive forces mostly enhance drainage time therefore it is not necessarily responsible for the decreased bubble size. The repulsive EDL can inhibit bubble coalescence by keeping the air-liquid interfaces away from

each other but upon addition of 0.01 M of salt the repulsive EDL became negligible and since most of the salt prevent bubble coalescence above this concentration this force cannot be responsible for the phenomena (Creux et al., 2007). The other repulsive force is the hydration pressure that arise from the bonded water molecules around the air-liquid interface and that only act from the distance of 5 – 6 Å therefore their influence is can not be significant (Israelachvili and Wennerstrom, 1996). An other explanation for the prevention of bubble coalescence is the decreased strength of the hydrophobic attraction force however there is not too much know about the length and magnitude of this force to fully explain the bubble coalescence prevention (Craig et al., 1993; Firouzi et al., 2015; Pugh and Yoon, 1994). The ion effect on air-liquid interface properties are focusing on the change of surface mobility that can be altered effectively even at small surface tension gradients (Klaseboer et al., 2000; Yaminsky et al., 2010). However in case of electrolyte solutions there are not enough evidence to prove this theory some studies showed that the surface mobility of bubbles in electrolyte solution close to the one observed in pure uncontaminated water solutions (Henry et al., 2008) while other works highlighted changes in the interface mobility in KCl solution while approaching solid surface (Parkinson and Ralston, 2010). The ion-pairs effect on bubble coalescence was studied extensively by Craig and co-authors (V. S. J. Craig, Ninham, & Pashley, 1993a; Vincent S.J. Craig, Ninham, & Pashley, 1993b). The anions and cations were separated into two categories, α and β, based on their effect on bubble coalescence. While αα and ββ electrolytes inhibit coalescence, the mixed combination of the two type electrolytes, αβ and βα, has no effect. The designations α and β are empirical based on the results of bubble coalescence experiments and they have not been successfully associated with any physical parameter of the ion. The ion pars effect on bubble coalescence was linked to the hydration level of the ion-pairs by Collins (Collins, 2004). Salts are built up of opposite charge of ions that relative radii size to each other can have a great effect on the hydration level of ion-pairs. It is considered that two strongly hydrated small ions (hard ions) of opposite charge or two weakly hydrated large ions (soft ions) of opposite charge would strongly attract to each other forming direct ion pairs that expelling the hydration water between them. When mixed ion-pairs (small – large) are in contact the large ion is not sufficient to make the small ion to lose its hydration shell so they remain apart from each other. Based on this matching ion-pair idea the bigger the different between the mixed ion-pairs the less successful the prevention of bubble coalescence.

Solid phase property

While particle size, liberation, shape and surface properties have a significant effect on the collision, attachment and detachment probability; there are certain particle properties that already affect the gas dispersion therefore affecting the collision probability by influencing the bubble size. These parameters are the particle size and chemical composition. Particles with the size smaller than 1 mm promote bubble coalescence that resulting bigger bubbles with higher rising velocity and therefore lower gas holdup while big particles promote bubble coalescence leading to smaller bubble size and hence higher gas holdup (Imafuku et al., 1968; Kato et al., 1972; Viswanthan et al., 1964). The dissolvent of the solid phase can modify the property and purity of the liquid phase resulting change in bubble size and rising velocity.

The current work focuses on parameters affecting bubble properties in two-phase (air-water) systems and compares the existing industrial methods used for monitoring bubble properties in flotation column.

HYDRODYNAMIC IN FLOTATION COLUMN

Gas dispersion parameters (Figure 2) are employed to determine how well the introduced air (Q_g) is distributed in the flotation machine. The introduced air will be distributed in the given cross section of the flotation machine (A_c) by forming air bubbles. As the result of the buoyancy force the bubbles will rise to the top of the cell but it rising velocity will be affected by the size (d_b) and shape of bubbles (Maldonado et al., 2013). As the bubble size decreases the rising velocity increases and resulting increase of air fraction in the air-liquid mixture. This ratio of gas fraction to liquid fraction is called gas-holdup (ε_g). These parameters together determine the active surface area where particle-bubble collision can take place and together with the particle floatability (P) will determine the flotation rate constant.

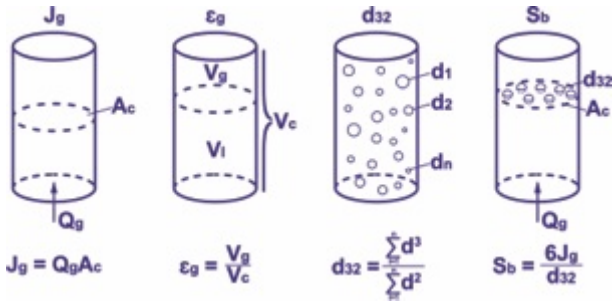


Figure 2. The four gas dispersion parameters used by industry to characterize how effectively the gas phase is dispersed in the liquid phase

Bubble size (d_b) and its rising velocity (U_t) together are the main factors determine the flow regime and therefore the hydrodynamic in the flotation column (Besagni and Inzoli, 2016) which govern the performance of bubble column reactor. Flow regime according to the structure of the gas holdup is either homogeneous or heterogeneous. The former indicate gentle mixing over the cross section of the column and associated with low superficial gas velocity (J_g). The bubbles in this flow regime are uniformly sized small bubbles with limited interactions and uninform U_t where the d_b is mostly determined by sparger (column design) and physical properties of the system (Hyndman et al., 1997; Thorat and Joshi, 2004) and it is frequently referred as bubble flow. The letter is the result of the increased J_g leading to more frequent bubble coalescence and broader bubble size distribution. The wide range of bubble size distribution leads to differences in U_t and hence to bubble segregation where bigger bubbles with higher U_t move to the centre of the column while smaller bubbles stay close to the wall of the column. The segregation phenomena is strongly depends on the size and shape of the bubbles (Sekoguchi et al., 1974).

It is crucial to bear in mind that the bubble size in the column is not necessary homogenous even in the homogenous zone. Homogenous zones can be either perfect, when the size of the bubbles are actually uniform and it is only possible if no coalescence occurs between the bubbles therefore the bubble size is determined by sparger system, or imperfect, when there is some variation in bubble size as a result of random bubble coalescence. Perfect bubble flow can be reached when the airflow rate is sufficiently low so there is no interaction between bubbles that would lead to coalescence or if the possible coalescence is prevented by the addition of sufficient amount of chemicals or impurities. In mineral processing these substances are flotation frothers or electrolytes. The concentration where the perfect bubbly flow is reached is called critical coalescence concentration (Cho and Laskowski, 2002), in case of flotation frothers, or transition concentration (Prince and

Blanch, 1990), in case of electrolytes. Imperfect bubbly flow forms when coalescence between the colliding bubbles can take place either due to the increased J_g or due to the insufficient frothers or electrolytes. The varying U_t across the cross section of the column is leading to internal circulation and turbulent eddies (energy cascade) encouraging further bubble-bubble coalescence and leading to slug flow that will result lover gas-liquid mass transfer coefficient in the column. Therefore the change from imperfect bubbly flow to slug flow is not just a function of increasing J_g as a function of ε_g and d_c as it was stated by Deckwer et al. (Deckwer et al., 1980) but also the function of the chemicals effect on bubble coalescence as a function of increasing turbulent intensity as it was highlighted by Javor and Filippov (Javor and Filippov, 2017).

In case of imperfect homogeneous system the determination of average bubble size is not that obvious as in case perfect homogeneous system. Determining only the mean bubble diameter (d_{10}) in imperfect homogeneous system can be misleading since it do not considers that not all bubbles has the same size or the same concentration. Therefore the Sauter mean diameter (d_{32}) was introduced (Hernandez-Aguilar et al., 2005) that is a surface, volume diameter that is suitably represents the whole imperfectly homogenous bubble population. Figure 3 demonstrates an average bubble size distribution can be obtained in an imperfect homogenous bubble flow.

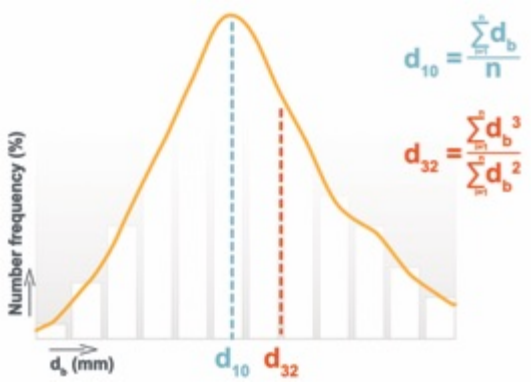


Figure 3. Mean diameters representing the whole size distribution of the bubbles

THE KEY PARAMETERS DETERMINE HYDRODYNAMIC IN FLOTATION COLUMN

Even though froth flotation is a three-phase process gas dispersion is often measured in two-phase systems. There are multiple reasons why studying two-phase systems is essential. The main reason is the complexity of the system. Already in two-phase system, the gas dispersions is affected by many factors (Figure 4) and some of them are still not well understood like the water quality effect that currently became a really important issue in mineral processing as the result of fresh water scarcity and increasing water demand (since the water requirement in froth flotation is determined by water to solid ratio the decreasing grade of the available minerals leading to the higher water demand).

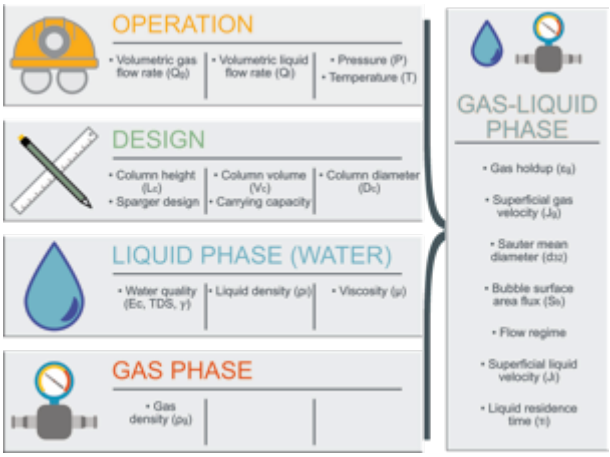


Figure 4. Schematic of the complexity of column flotation in 2-phase system

Linking the obtained two-phase system data to three-phase system data is not easy since the solid already affects the property of the liquid phase and consequently the hydrodynamic in the column therefore the interactions between the five major parameters affecting column operation have to be understood perfectly (Figure 5).

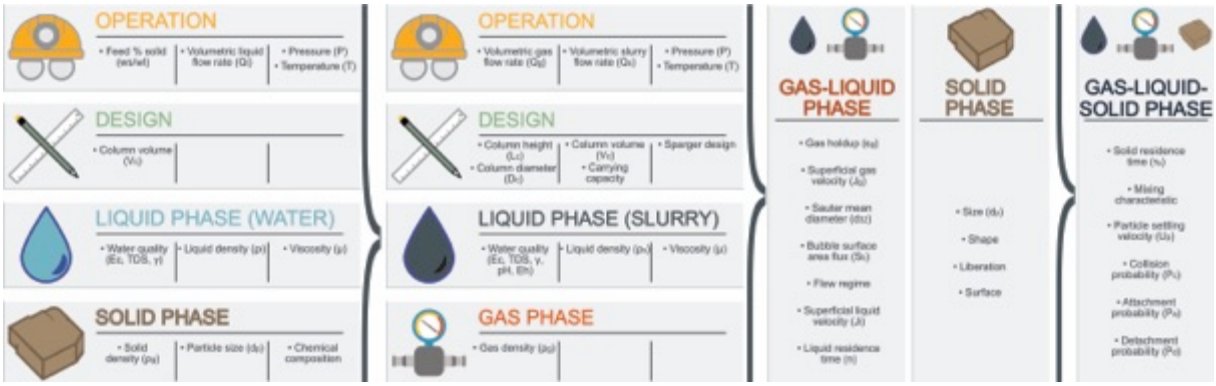


Figure 5. Schematic of the complexity of column flotation in 3-phase system

MEASURING OF BUBBLE SIZE

There are multiple methods used for determining bubble size in flotation column, however these methods can be divided into two major groups based on the data extraction routine: direct and indirect method.

The direct method allows measuring the bubbles one by one so the bubble size distribution can be precisely determined however to do so the bubble population in the column have to be sampled and extracted one by one. The sampling process can disturb column operation and hence affecting on the obtained results. Additional errors arise as the result of bubble extraction such as the change in volume due to the increase in vertical displacement, the change in coalescence probability due to the restricted lateral movement and increased manipulation of the bubbles (Sovechles and Waters, 2015). Other disadvantage of the direct method is the expansive and sensitive instrumentation that usually associated with these methods that many time do not suitable for industrial conditions and can be challenging to use it during continuous operation. Machine vision technique (Grau and Heiskanen, 2002; Hernandez-Aguilar et al., 2002) is the most widely used direct method where the

bubbles are collected with a sampling tube and ushered into a glass or acryl bubble viewer. The bubble viewer is placed between a photo camera and a backlight so the rising bubbles can be imaged against a backlight highlighting the silhouette of the bubbles. Other popular indirect methods are: optical fibre (Besagni and Inzoli, 2016; Chabot et al., 1998; Moujaes, 1990; Tucker et al., 1994), acoustic method (Kracht and Moraga, 2016) and double sensor conductivity probe (Wu et al., 2001).Optical fibre operate based on the difference in reflective index, or conductive respectively of the gas and liquid phase measuring local holdup, bubble chord length and rise velocity. In mineral processing the most commonly used optical sensor is the UCT bubble probe (Tucker et al., 1994) that collect the bubbles via a sampling capillary and deformed them to a cylinder and measure the chord length. The narrow size of the sampling capillary is inevitable in three phase system operation so no particles will collected in the sampling capillary. The acoustic method data collection method is similar to the machine vision technique. The bubbles collected from the column is ushered into an acoustic chamber where a mixed signal of a carrying signal and a modulating signal is transmitted to the water and the bubbles are responding to this signal and the respond signal is received by a transducer and from the different between the transmitted and received signal the bubble size can calculated. The great benefit of the acoustic technique over the machine vision technique is the lack of expensive imaging tools (CCD camera and back light). Double sensor conductivity probe can measure the conductivity difference between the bubbles and the slurry without collecting and extracting the bubbles from the system however the probe only detect the bubbles that are directly in contact with.

The indirect method includes measurement techniques where data are collected from a cross section of the column with sensors that have no direct effect on the operation of the column. The great benefit of these methods that it can be used in continuous operation without disturbing or affecting the process but on the down side it do not provide visual confirmation and the obtained bubble size data is the result of a numerical calculation. The most commonly employed sensors for indirect bubble size analyses are the pressure (Finch and Dobby, 1990) and conductivity (Gomez and Finch, 2007) sensors. The sensors detect the gas-holdup and the bubble size is iterated based on the correlation between the bubble size and its rising velocity. Such numerical calculation method is called drift flux (DF) analyse. The acoustic sensors (Spencer et al., 2012) are also employed in column flotation where the bubble size is determined as a function of resonance frequency (f_0). There are other indirect techniques that are suitable for gas holdup measurements without disturbing the system but these techniques just like the direct methods require expansive and sensitive instrumentation that has a huge additional space requirement and many times do not suitable for industrial conditions. Such techniques are the γ ray tomography (Kumar et al., 1995) or the laser Doppler anemometer (Kulkarni et al., 2001).

COMPARING THE NUMBERING AND IMAGING ANALYSING TECHNIQUES

The experimental setup

A 5.5 m high pilot size flotation column with an inner diameter of 0.075 m was used during the experimental work Figure 6 (Filippov et al., 2000). Two sparger systems are installed on the column (Microcell™ (Metso) and a modified Slamjet® called Flotaire (Deister Concentrator)) that can be changed between two experimental works. In this current work the Flotaire sparger system was employed. A centrifugal Dyton pump located at the bottom of the column was employed to circulate

the air/water mixture via the sparger. Airflow rate is reported as a superficial gas velocity (J_g) and the feed rate as superficial liquid velocity (J_l). The J_g and J_l was set to 0.85 cm/s and 1.14 cm/s respectively.

Two Masterflex pumps are used as a feed and a tailing pump. The two pumps were connected so if the feed rate or gas holdup changed the tailing pump speed was modified automatically to keep the liquid level constant in the column.

Two Rosemount 300S pressure sensors (P_1, P_2,) are placed 2.0 m apart was used to determine gas holdup and bubble size in this given section of the flotation column using drift flux model. A bubble viewer was installed at the upper part of the cell and the bubbles were sampled above the P_1 sensor. The sampling point of the viewer can be modified so bubble population close to the wall or in the centre of the column can be monitored. The sampling tube is installed in 45º and its inner diameter is 10 mm. The collected bubbles were later released into the column close to the feeding point.

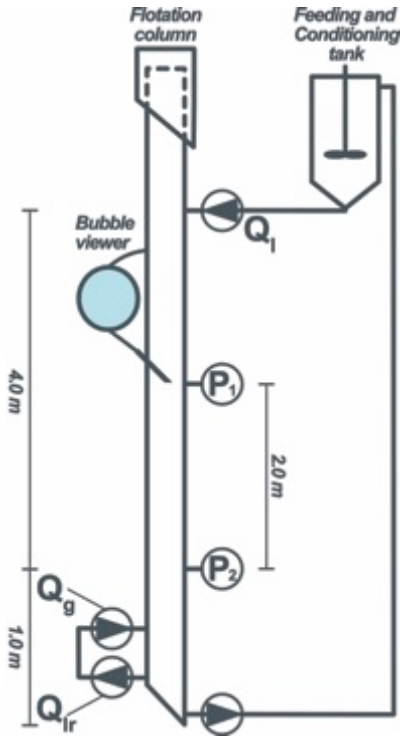


Figure 6. The schematic of the 5.5 m high experimental setup used during the experimental work

During a set of measurement 40 L of 10 ppm MIBC solution was prepared in the feeding tank before introducing into the column. The 10 ppm MIBC is at the level of typical plant operations but still below the so called critical coalescence concentration (Gélinas and Finch, 2007; Quinn et al., 2014, 2007). After 30 min of closed circuit column operation the J_l and J_g was set and the pressure change was recorded in every 6 s for 20 min. Therefore, each set of measurement included 201 measured ΔP data that was used to calculate average gas holdup and average Sauter mean bubble size (d_{32}).

Pressure sensors – Drift flux analysis

Using drift flux analysis bubble size can be estimated from measured ε_g, J_g and J_l. The core assumption of the drift flux analysis is that the bubble size is uniform and that the slip velocity of the gas and liquid phase in a counter current system is defended by:

$$U_{sg} = \frac{J_g}{\varepsilon_g} + \frac{J_l}{(1-\varepsilon_g)}$$

while the slip velocity of one single bubble (U_T) is related to U_{sg} (Richardson and Zaki, 1954):

$$U_{sg} = U_T(1-\varepsilon_g)^{m-1}$$

where m is a function of the Reynolds number of a single bubble:

$$m = \left(4.45 + 18\frac{d_b}{d_{column}}\right) Re_b^{-0.1} \qquad for\ 1 < Re_b < 200$$

$$m = 4.45\ Re_b^{-0.1} \qquad for\ 200 < Re_b < 500$$

$$Re_b = \frac{d_b U_T \rho_l}{\mu_l}$$

An alternative equation (a semi-empirical) was developed by Filippov (Filippov, 1996) to determine U_T using the experimental data of Clift et al.(Clift et al., 1978):

$$U_{T*} = 3 \cdot 10^6 d_b^3 - 36420 d_b^2 + 150.58 d_b - 0.007$$

where db is a function of the Reynolds number in a swarm:

$$d_b = \left(\frac{18\mu_f U_t}{g\Delta\rho}(1 + 0.15 Re_s^{0.687})\right)^{1/2}$$

$$Re_s = \frac{d_b U_{sg} \rho_l (1-\varepsilon_g)}{\mu_l}$$

There are different iterations routines can be applied to determine bubble size. The present study introduces four methods (Figure 7): Yianatos et al. (Yianatos et al., 1988); Dobby et al. (Dobby et al., 1988); Xu & Finch (Banisi and Finch, 1994) and Filippov (Filippov, 1996).

As it was mentioned above the core assumption of this method is that the bubble size distribution is perfectly homogeneous however this is only the case if no coalescence is possible between colliding bubbles in the flotation column. This would occur when the airflow rate is too low so the collision probability is almost zero or in case of high frother concentration (above the critical coalescence concentration) or electrolyte concentration (transition concentration). However below these critical concentrations the frother/surfactant has a significant effect on bubble size distribution meaning that identical Sauter mean diameter could be the result of two unalike bubble size distribution (Javor et al., 2016)).

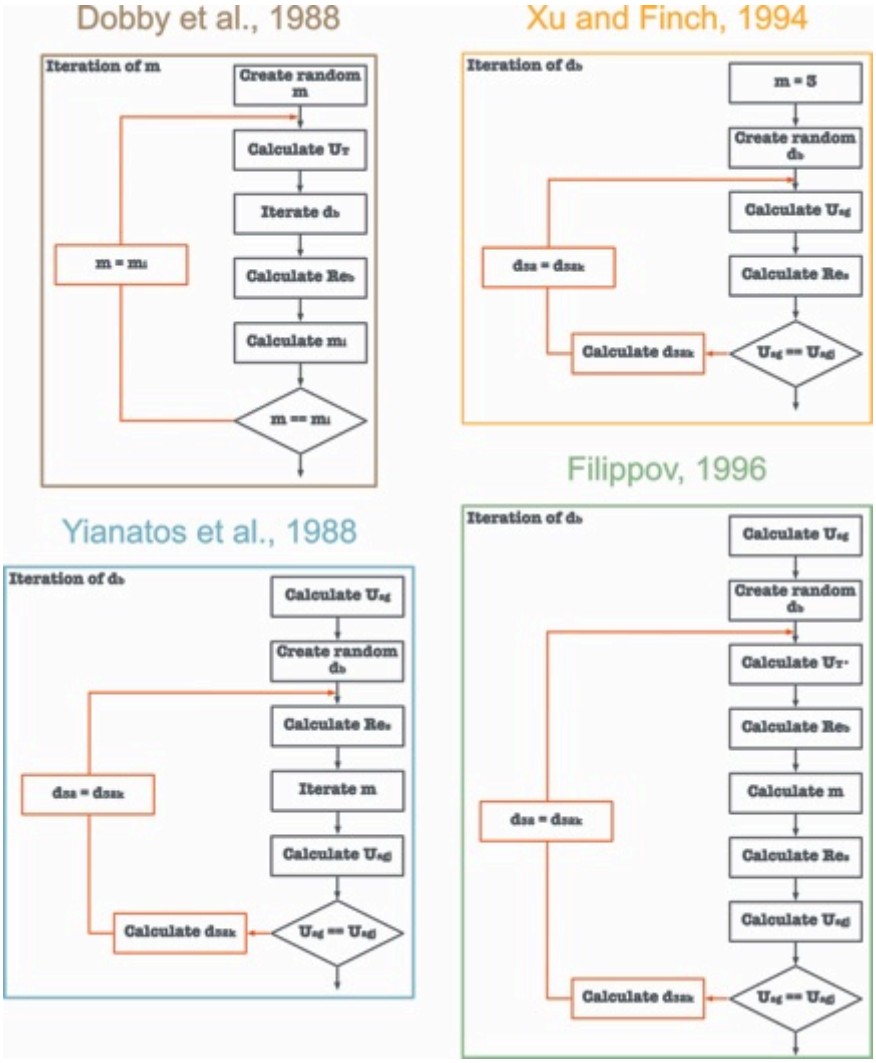


Figure 7. Flowcharts of the four numerical methods used to calculate bubble diameter based on pressure differences

Population balance models are designed to predict bubble size distribution using numerical calculation. These models have to describe the bubble-bubble interactions such as bubble coalescence and breakage in dynamic condition. This is a really complex challenge since both coalescence and breakage is strongly influenced by operational parameters, design parameters, continuous phase properties and dispersed phase properties.

Machine vision or image analysis method

Digital image capturing and analysis is a commonly used method to determine bubble size. The main concept is to collect bubbles from the flotation machine via a sampling tube and usher it to a bubble viewer where the image capturing takes place. The bubbles imaged against a backlight so the silhouette of the bubbles are well defined. The employment of image analysis method can introduce many additional errors including resolution, number of captured bubbles (statistically meaningful data set is required), or shape identification (Sovechles and Waters, 2015).

McGill bubble viewer is a commercialized bubble sampling and image capturing system that is extensively used by industry for bubble size measurement. However for image analyses there is no commonly accepted image analyses process. There are many different methods for image analyses however all these methods has different image processing routines. The three most commonly used

image analyses software are: the commercially available Northern Ecliple, the open source ImageJ and Matlab scripts that mostly developed by different research institutes and laboratories. The basic shape analysis method is the ellipse fitting (or circular particle detection) however this method is not always efficient (Figure 8) especially in case of bubble clusters. Northern Eclipse offers a fully automatized image analysis commercial package however based on Miskovic and Luttrel (Miskovic and Luttrell, 2012) the software only recognize 5 to 40 % of bubbles found in clusters. This is a great challenge in image analysing to recognize bubbles that are closely packed and overlapping each other. There are various image processing routines introduced to tackle this challenge: Hough transforms (Riquelme-Diaz, 2014), Watershed transform (this transform is a build in function of ImageJ), breakpoint method (Fu and Liu, 2016). Friberg et al. (Friberg et al., 2017) collected the limitations of all the above-introduced routines and developed a new image processing routine that is capable of segmenting 97.7% of the bubbles found in clusters (Gaussian mixed model is used to separate the cluster for single bubbles).

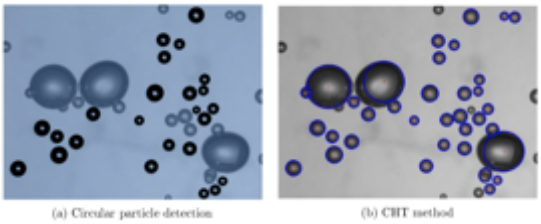


Figure 8. Detection of cluster bubbles with two different image processing routines (circular particle detection and circular Hough algorithm

RESULTS AND DISCUSSION

Pressure sensors – Drift flux analysis

The pressure differences between P1 and P2 were monitored online for 20 minutes and in each sixth second the measured data was saved into an excel file. The recorded 201 ΔP data was later processed using the four numerical drift flux calculations introduced above. For each recorded ΔP the bubble size was iterated and it was printed as a function of time on Figure 9. All of the bubble size following the same pattern as a function of time and all of the numerical calculation method predicted really similar bubble size (1.0 ± 0.06 mm).

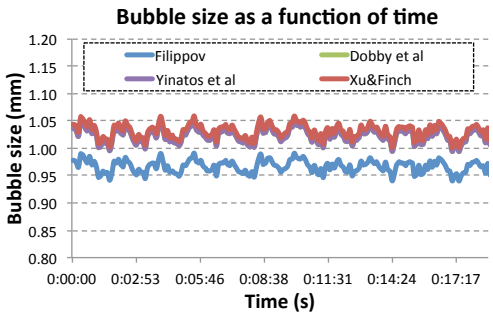


Figure 9. Bubble size as a function of time calculated by different numerical methods (Banisi and Finch, 1994; Dobby et al., 1988; Filippov, 1996; Yianatos et al., 1988)

The average of all the iterated parameters is introduced in Table 1. The calculation of Yianatos et al. (Yianatos et al., 1988) and Dobby et al. (Dobby et al., 1988) gives identical result since the only difference between the two iteration processes is the "starting point" of the iteration (basically one is the reorganised version of the other). The other two numerical methods (Banisi and Finch, 1994; Filippov, 1996) shows some differences since both use some simplification. The simplification of Xu and Finch, which assumes that 'm' is constantly 3, generates relatively small deviation in this case from the data obtained by Yianatos et al. and Dobby et al. The simplification of Filippov, which assumes that each bubbles terminal velocity is can be determined based on its diameter using a semi-empirical model, causes a bit bigger deviation but still provides a really accurate bubble size data.

Table 1. The average gas holdup (ε_g), slip velocity (U_t), Reynolds numbers (Re_b and Re_s) and Sauter mean diameter (d_{32}) calculated by the different numerical drift flux method.

Drift flux method	ε_g (%)	U_t (m/s)	Re_b	m	Re_s	d_{32} (mm)
Filippov (1996)	9.13	0.11	104	2.94	78	0.97
Dobby et al. (1988)	9.13	0.13	130	2.89	98	1.02
Yinatos et al. (1988)	9.13	0.13	130	2.89	98	1.02
Xu and Finch (1994)	9.13	0.13	132	3.00	99	1.03

Machine vision or image analysis method

Fifteen pictures in every 2 minutes were captured randomly during the 20 minutes of measurement time. The captured 165 pictures were first batch processed by Affinity Photo to enhance contrast and format them into grayscale images. The grayscale pictures were analysed by four different image analysing routines: Northern Eclipse, Hough transforms, Watershed transform and Gaussian mixed model. Figure 10 shows the determined bubble size distribution obtained by the different image analysing routines.

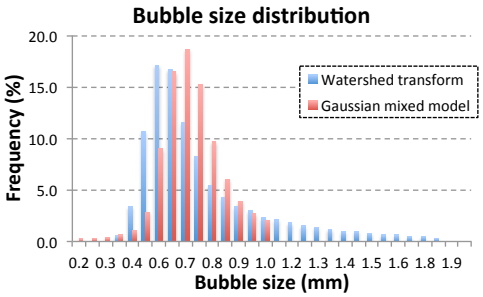


Figure 10. Bubble size distribution determined by different image analyzing routines

The size distributions curves show close similarity even though there is a small shift between them. However, if we investigate the number of bubbles detected by the different routines and the calculated Sauter mean diameter a huge different can be observed (Table 2). The Gaussinan mixed model detected almost 2 times as much bubbles as the Watershed transform that could be the result of the better cluster segmentation process.

It is also worth to notice that the calculated d_{32} results are much higher than the one expected based on the drift flux analyses or the bubble size distribution data. The obtained high d_{32} caused by some unusually big bubbles that frequency is low but its volume is significant has a pronounced effect on the surface, volume diameter (d_{32}). These big bubbles can be the result of the inaccurate cluster

analyses or some “side-effect” of the sampling process. Table 2 also collecting the number of bubbles (and there size range) that had to be ignored to obtained similar d_{32} data as it was expected based on the Drift flux analyses. These data suggest that even a few bubbles can affect the calculated d_{32} significantly even in case of an extremely accurate cluster segmentation routine like the Gaussian mixed model. The data also show that the less accurate the segmentation routine the less bubble is recognised and the more bubbles have to be filtered to reach the desired d_{32}, therefore with each image processing routine different baseline is required for maximum bubble size which is impossible to predict alone by image analysing data.

Table 2. Number of detected bubbles and d32 obtained by different image analyses methods

Image analyses method	Number of detected bubbles	d_{32} (mm)	Number of filtered bubbles	Filtrated size range	d_{32} filtered (mm)
Northern Eclipse	NA	NA	NA	NA	NA
Hough transforms	NA	NA	NA	NA	NA
Watershed transform	44.251	1.54	1.657	> 2.0 mm	0.98
Gaussian mixed model	94.898	1.33	512	> 2.8 mm	0.98

CONCLUSION

The results highlighted that the numerical data processing is not particularly sensitive to the analysing routine used to iterate bubble size. Therefore with this indirect measurement method accurate date can be obtained consistently making it an easy and suitable for industrial condition. On the other hand there is no accurate numerical method to estimate bubble size distribution.

The direct image analysing technique highlighted that the sampling process and also the data analysing routines has a significant effect on the obtained bubble size data makes challenging to use it as an industrial method. However it provides a really detailed size distribution data that can be extremely useful in operation adjustment in case there is no error made during date sampling and analysing.

ACKNOWLEDGEMENT

The authors extend their appreciation to Ms. Caroline Izart (Université de Lorraine) for her useful advices on the drift flux analyses scripts. Special thanks Mr. Tapio Freiberg (Aalto University), Mr. Mark Lepage (McGill University) and Dr. Miguel Maldonado (Universidad de Santiago de Chile) for their support and help with the different image analysing techniques.

The authors acknowledge French National Research Agency through the ‘Investissements d’avenir’ national research program LabEx RESSOURCES21 (ANR–10–LABX–21-01) and H2020 FAME project “Flexible and mobile processing technology for processing of skarn, greisen and pegmatite ores in Europe” (grant agreement No 641650) for partial financial support.

REFERENCES

Banisi, S., Finch, J.A., 1994. Technical note reconciliation of bubble size estimation methods using drift flux analysis. Miner. Eng. 7, 1555–1559. doi:10.1016/0892-6875(94)90046-9

Besagni, G., Inzoli, F., 2016. Comprehensive experimental investigation of counter-current bubble column hydrodynamics: Holdup, flow regime transition, bubble size distributions and local flow properties. Chem. Eng. Sci. 146, 259–290. doi:10.1016/j.ces.2016.02.043

Chabot, J., Farag, H., de Lasa, H., 1998. Fluid dynamics of bubble columns at elevated. temperature modelling and investigation with refractive fibex optic sensors. Chem. Eng. J. 70, 105–113.

Cho, Y.S., Laskowski, J.S., 2002. Effect of flotation frothers on bubble size and foam stability. Int. J. Miner. Process. 64, 69–80. doi:10.1016/S0301-7516(01)00064-3

Clift, R., Grace, J.R., Weber, M.E., 1978. Bubbles, Drops, and Particles. Academic Press, INC., New York.

COCHILCO, 2009. Best practices and efficient use of water in the mining industry.

Craig, V.S.J., Ninham, B.W., Pashley, R.M., 1993. The Effect of Electrolytes on Bubble Coalescence in Water. J. Phys. Chem. 97, 10192–10197. doi:10.1021/j100141a047

Creux, P., Lachaise, J., Graciaa, A., Beattie, J.K., 2007. Specific Cation Effects at the Hydroxide-Charged Air / Water Interface. J. Phys. Chem. C 111, 3753–3755.

Deckwer, W.-D., Louisi, Y., Zaidi, A., Ralek, M., 1980. Hydrodynamic Properties of the Fischer-Tropsch Slurry Process. Ind. Eng. Chem. Process Des. Dev. 19, 699–708. doi:10.1021/i260076a032

Dobby, G.S., 2002. Column flotation, SGS Minerals Services.

Dobby, G.S., Yianatos, J.B., Finch, J.A., 1988. Estimation of bubble diameter in flotation columns from drift flux analysis. Can. Metall. Q. 27, 85–90. doi:10.1179/cmq.1988.27.2.85

Filippov, L., 1996. Flotation de fines particules et de precipite organometallique en colonne. Université de Lorraine.

Filippov, L.O., Joussemet, R., Houot, R., 2000. Bubble spargers in column flotation: Adaptation to precipitate flotation. Miner. Eng. 13, 37–51. doi:10.1016/S0892-6875(99)00148-X

Finch, J.A., Dobby, G.S., 1990. Column Flotation. Pergamon Press.

Firouzi, M., Howes, T., Nguyen, A. V., 2015. A quantitative review of the transition salt concentration for inhibiting bubble coalescence. Adv. Colloid Interface Sci. 222, 305–318. doi:10.1016/j.cis.2014.07.005

Friberg, T., Schreithofer, N., Serna-Guerrero, R., 2017. A robust image processing routine for bubble size measurment in flotation machines and chemical reactors.

Fu, Y., Liu, Y., 2016. Development of a robust image processing technique for bubbly flow measurement in a narrow rectangular channel. Int. J. Multiph. Flow 84, 217–228. doi:10.1016/j.ijmultiphaseflow.2016.04.011

Gélinas, S., Finch, J.A., 2007. Frother analysis : Some plant experiences. Miner. Eng. 20, 1303–1308. doi:10.1016/j.mineng.2007.07.008

Gomez, C.O., Finch, J.A., 2007. Gas dispersion measurements in flotation cells. Int. J. Miner. Process.

84, 51–58. doi:10.1016/j.minpro.2007.03.009

Grau, R.A., Heiskanen, K., 2002. Visual technique for measuring bubble size in flotation machines. Miner. Eng. 15, 507–513. doi:10.1016/S0892-6875(02)00074-2

Henry, C.L., Dalton, C.N., Scruton, L., Craig, V.S.J., 2007. Ion-Specific Coalescence of Bubbles in Mixed Electrolyte Solutions. J. Phys. Chem. C 111, 1015–1023. doi:10.1021/jp066400b

Henry, C.L., Parkinson, L., Ralston, J.R., Craig, V.S.J., 2008. A Mobile Gas - Water Interface in Electrolyte Solutions. J. Phys. Chem. Lett. C 112, 15094–15097. doi:10.1021/jp8067969

Hernandez-Aguilar, J.R., Gomez, C.O., Finch, J.A., 2002. A technique for the direct measurement of bubble size distributions in industrial flotation cells, in: 34th Annual Meeting of the Canadian Mineral Processor. Ottawa, pp. 389–395.

Hernandez-Aguilar, J.R., Rao, S.R., Finch, J.A., 2005. Testing the k – S b relationship at the microscale. Miner. Eng. 18, 591–598. doi:10.1016/j.mineng.2004.10.003

Hyndman, C.L., Larachi, F., Guy, C., 1997. Understanding gas-phase hydrodynamics in bubble columns: A convective model based on kinetic theory. Chem. Eng. Sci. 52, 63–77. doi:10.1016/S0009-2509(96)00387-9

Imafuku, K., Wang, T.-Y., Koide, K., Kubota, H., 1968. The behaviour of suspended solid perticles in teh bubble column. J. Chem. Eng. Japan 1, 153–158.

Israelachvili, J., Wennerstrom, H., 1996. Role of hydration and water structure in biological and colloidal interactions. Nature 379, 219–225.

Javor, Z., Filippov, L.O., 2017. Salt effect on gas dispersion in flotation column - Bubble size as a function of flotation column height.

Javor, Z., Schreithofer, N., Heiskanen, K., 2016. Multi-scale analysis of the effect of surfactants on bubble properties. Miner. Eng. 99, 170–178. doi:10.1016/j.mineng.2016.09.026

Kantarci, N., Borak, F., Ulgen, K.O., 2005. Bubble column reactors. Process Biochem. 40, 2263–2283. doi:10.1016/j.procbio.2004.10.004

Kara, S., Kelkar, B.G., Shah, Y.T., Carr, N.L., 1982. Hydrodynamics and Axial Mixing in a Three-phase Bubble Column. Ind. Eng. Chem. Process Des. Dev. 21, 584–594.

Kato, Y., Nishiwaki, A., Fukuda, T., Takana, S., 1972. The behavior of suspended solid particles and liquid in bubble columns. J. Chem. Eng. Japan 5, 112–118.

Klaseboer, E., Chevaillier, J.P., Gourdon, C., Masbernat, O., 2000. Film Drainage between Colliding Drops at Constant Approach Velocity: Experiments and Modeling. J. Colloid Interface Sci. 229, 274–285. doi:10.1006/jcis.2000.6987

Kracht, W., Moraga, C., 2016. Acoustic measurement of the bubble Sauter mean diameter d 32. Miner. Eng. 98, 122–126. doi:10.1016/j.mineng.2016.08.001

Kulkarni, A.A., Joshi, J.B., Kumar, V.R., Kulkarni, B.D., 2001. Application of multiresolution analysis for simultaneous measurement of gas and liquid velocities and fractional gas hold-up in bubble column using LDA. Chem. Eng. Sci. 56, 5037–5048.

Kumar, S.B., Moslemian, D., Dudukovi, M.P., 1995. A y-ray tomographic scanner for imaging voidage distribution in two-phase flow systems. Flow Meas. Instrum. 6, 61–73.

Maldonado, M., Quinn, J.J., Gomez, C.O., Finch, J.A., 2013. An experimental study examining the relationship between bubble shape and rise velocity. Chem. Eng. Sci. 98, 7–11. doi:10.1016/j.ces.2013.04.050

Miskovic, S., Luttrell, G.H., 2012. Comparison of two bubble sizing methods for performance evaluation of mechanical flotation cells. Technol. Miner. Coal Earth Resour. 563–574.

Moujaes, S.F., 1990. Testing of a Spherical Dual-tipped Optical Fiber Probe for Local Measurements of Void Fraction and Gas Velocity in Two-Phase Flows. Can. J. Chem. Eng. 68, 504–510.

Pangarkar, V.G., 2015. Design of Multiphase Reactors. John Wiley & Sons, Inc.

Parkinson, L., Ralston, J., 2010. The Interaction between a Very Small Rising Bubble and a Hydrophilic Titania Surface. J. Phys. Chem. C 114, 2273–2281.

Pino, L.Z., Solari, R.B., Siquier, S., Estévez, L.A., Yépez, M.M., Sáez, A.E., 1992. Effect of operating conditions on gas holdup in slurry bubble columns with a foaming liquid. Chem. Eng. Commun. 117, 367–382.

Prince, M.J., Blanch, H.W., 1990. Transition electrolyte concentrations for bubble coalescence. AIChE J. 36, 1425–1429. doi:10.1002/aic.690360915

Pugh, R.J., Yoon, R.-H., 1994. Hydrophobicity and rupture of thin aqueous films. J. Colloid Interface Sci. 163, 169–176.

Quinn, J.J., Kracht, W., Gomez, C.O., Gagnon, C., Finch, J. a., 2007. Comparing the effect of salts and frother (MIBC) on gas dispersion and froth properties. Miner. Eng. 20, 1296–1302. doi:10.1016/j.mineng.2007.07.007

Quinn, J.J., Sovechles, J.M., Finch, J.A., Waters, K.E., 2014. Critical coalescence concentration of inorganic salt solutions. Miner. Eng. 58, 1–6. doi:10.1016/j.mineng.2013.12.021

Richardson, J.F., Zaki, W.N., 1954. Sedimentation and fluidisation: Part I. Chem. Eng. Res. Des. 75, S82–S100. doi:10.1016/S0263-8762(97)80006-8

Riquelme-Diaz, A., 2014. Bubble size distribution measurement , modeling and control in a laboratory flotation column. Universite Laval.

Sastri, S., 1998. Column Flotation • Theory and Practice. Froth Floatation Recent Trends 44–63.

Schafer, R., Merten, C., Eigenberger, G., 2002. Bubble size distributions in a bubble column reactor under industrial conditions. Exp. Therm. Fluid Sci. 26, 595–604.

Sekoguchi, K., Nishikawa, K., Nakasatomi, M., Hirata, N., Higuchi, H., 1974. Flow boiling in subcooled and low quality regions - heat transfer and local void fraction, in: International Heat Transfer Conference 5. Tokyo, Japan, pp. 180–184.

Serizawa, A., Kataoka, I., Michiyoshi, I., 1975. Turbulence structure of air-water bubbly flow-II. local properties. Int. J. Multiph. Flow 2, 235–246. doi:10.1016/0301-9322(75)90012-9

Shah, Y.T., Kelkar, B.G., Godbole, S.P., Deckwer, W.-D., 1982. Design parameters estimations for bubble column reactors. AIChE J. 28, 353–379. doi:10.1002/aic.690280302

Sovechles, J.M., Waters, K.E., 2015. Effect of ionic strength on bubble coalescence in inorganic salt and seawater solutions. AIChE J. 61, 2489–2496. doi:10.1002/aic

Spencer, S.J., Bruniges, R., Roberts, G., Sharp, V., Catanzano, A., Bruckard, W.J., Davey, K.J., Zhang, W., 2012. An acoustic technique for measurement of bubble solids mass loading: (b) Monitoring of Jameson cell flotation performance by passive acoustic emissions. Miner. Eng. 36–38, 21–30. doi:10.1016/j.mineng.2012.02.011

Thorat, B.N., Joshi, J.B., 2004. Regime transition in bubble columns: Experimental and predictions. Exp. Therm. Fluid Sci. 28, 423–430. doi:10.1016/j.expthermflusci.2003.06.002

Tucker, J.P., Deglon, D.A., Franzidis, J.P., Harris, M.C., O'Connor, C.T., 1994. An evaluation of a direct method of bubble size distribution measurement in a laboratory batch flotation cell. Miner. Eng. 7, 667–680. doi:10.1016/0892-6875(94)90098-1

Viswanthan, S., Kakar, S., Murti, P.S., 1964. Effect of dispersing bubbles into liquid fluidized beds on heat transfer and hold-up at constant bed expansion. Chem. Eng. Sci. 20, 903–910.

Wills, B.A., Finch, J.A., 2015. Froth Flotation, in: Will's Mineral Processing Technology. pp. 457–595. doi:10.1016/B978-0-08-034937-4.50021-1

Wu, Q., Welter, K., Mccreary, D., Reyes, J.N., 2001. Theoretical studies on the design criteria of double-sensor probe for the measurement of bubble velocity 12, 43–51.

Yaminsky, V. V., Ohnishi, S., Vogler, E.A., Horn, R.G., 2010. Stability of aqueous films between bubbles. Part 1. the effect of speed on bubble coalescence in purified water and simple electrolyte solutions. Langmuir 26, 8061–8074. doi:10.1021/la904481d

Yianatos, J.B., Finch, J.A., Dobby, G.S., Xu, M., 1988. Bubble size estimation in a bubble swarm. J. Colloid Interface Sci. 126, 37–44. doi:10.1016/0021-9797(88)90096-3